Heliyon 10 (2024) e38421

Contents lists available at ScienceDirect

Heliyon

journal homepage: www.cell.com/heliyon

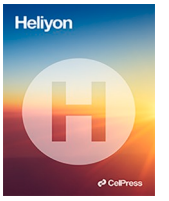

Research article

Maidong Dishao Decoction mitigates submandibular gland injury in NOD mice through modulation of gut microbiota and restoration of Th17/Treg immune balance

Yue Zhang [a], Yunxia Wu [a], Yin Guan [a], Yun Lu [a], Wen Zhu [b,**], Fan Ping [c,***], Yue Wang [b,*]

[a] The First Clinical Medical College, Nanjing University of Chinese Medicine, Nanjing, China
[b] Affiliated Hospital of Nanjing University of Chinese Medicine, Jiangsu Province Hospital of Chinese Medicine, Nanjing, China
[c] Jiangsu Health Vocational College, Nanjing, China

ARTICLE INFO

Keywords:
Primary Sjogren's syndrome
Maidong Dishao Decoction
Th17/Treg immune balance
Submandibular gland
Gut microbiota

ABSTRACT

Background: Primary Sjogren's syndrome (pSS) is a common chronic autoimmune disease that presents limited treatment options and poses significant challenges for patients. Maidong Dishao Decoction (MDDST), a traditional Chinese medicine compound, has demonstrated potential in alleviating dryness symptoms associated with pSS. Therefore, it is important to study the specific mechanism of its therapeutic effect.

Objective: This study aims to investigate the effects of MDDST on gut microbiota, short-chain fatty acids (SCFAs), and the Th17/Treg immune balance in non-obese diabetes (NOD) mice.

Methods: The study employed ultrahigh-performance liquid chromatography coupled with quadrupole-exactive mass spectrometry (UHPLC-QE-MS) to identify the primary components of MDDST. Subsequently, hematoxylin and eosin (HE) staining, enzyme-linked immunosorbent assays (ELISA), and flow cytometry analyses were conducted to evaluate the therapeutic effects of MDDST in NOD mice. Additionally, 16S rDNA sequencing and gas chromatography-mass spectrometry (GC-MS) were utilized to assess the influence of MDDST on gut microbiota and SCFAs. Finally, fecal microbiota transplantation (FMT) and SCFA-based interventions were performed to elucidate the mechanisms through which MDDST exerts its effects.

Results: The research findings demonstrate that MDDST exerts therapeutic effects on NOD mice, primarily manifested as reduced inflammation, decreased water intake, ameliorated pathological changes and lowered levels of Sjogren's syndrome antigen A (SSA) and immunoglobulin G (IgG). Additionally, MDDST significantly decreased serum levels of interleukin-6 (IL-6) and interleukin-17 (IL-17), while enhancing levels of interleukin-10 (IL-10) and transforming growth factor beta (TGF-β), thereby regulating the Th17/Treg immune balance. Further investigations revealed that MDDST treatment induces alterations in gut microbiota composition and elevates SCFA levels in the gut. Subsequent FMT and SCFA intervention experiments demonstrated a downregulation of pSS-related phenotypes.

* Corresponding author.
** Corresponding author.
*** Corresponding author.
E-mail addresses: zhuwen@njucm.edu.cn (W. Zhu), fping@jshvc.edu.cn (F. Ping), wangyue@njucm.edu.cn (Y. Wang).

https://doi.org/10.1016/j.heliyon.2024.e38421
Received 2 April 2024; Received in revised form 18 September 2024; Accepted 24 September 2024
Available online 25 September 2024

Conclusion: In summary, MDDST demonstrates protective effects against pSS by restoring the balance between Th17 and Treg cells. The therapeutic effects can be partially attributed to its regulation of gut microbiota and SCFAs. Our finding provides a new option for treating pSS.

1. Introduction

Primary Sjogren's syndrome (pSS) is a common chronic autoimmune disease characterized by inflammation and damage to the salivary and lacrimal glands [1]. This condition frequently leads to considerable discomfort due to dry mouth and dry eyes, significantly impacting the individual's quality of life [2]. The incidence rate of pSS has been increasing progressively [3], yet there is no established effective treatment currently available. However, traditional Chinese medicine (TCM) has shown promising results in managing pSS, offering notable therapeutic benefits with minimal side effects. As a result, it has been widely utilized in China.

Recently, studies have emphasized the significant role of gut microbiota in the pathogenesis of pSS [4]. The dysbiosis of gut microbiota is closely associated with systemic inflammation [5–7] and it has been observed that gut microbiota and its metabolites can modulate the host immune system [8–13]. Metabolites present in the intestinal tract, particularly short chain fatty acids (SCFAs), are known to play pivotal roles in immune regulation. For instance, acetate and propionate have demonstrated a capacity to downregulate T helper 17 cell (Th17) expression and IL-17 production [14,15]. Furthermore, propionate and butyrate have been found to enhance regulatory T cell (Treg) generation [16–18]. Therefore, investigating the interplay between gut microbiota, SCFAs and Th17/Treg immune balance holds immense significance in acquiring a deeper comprehension of the underlying mechanism behind pSS disease.

Maidong Dishao Decoction (MDDST), a traditional Chinese medicine compound used in clinical practice to treat dryness syndrome, is formulated based on the traditional Chinese medicine theory of the 'Exterior-interior Relationship between the Lung and Large Intestine' [19]. The herbs of MDDST (Table S1) include Maidong (dwarf lilyturf tuber), Dihuang (rehmannia root), Baishao (white peony root), Taoren (peach seed) and Ziwan (tatarian aster root). Clinical studies have shown that MDDST can improve salivary and lacrimal gland dysfunction in patients with pSS, as well as alleviate dryness symptoms, mainly due to its anti-inflammatory properties [20,21]. Moreover, the active ingredients of the main drugs in MDDST have been found to have therapeutic effects on pSS animal models by regulating interplay between T and B cells [22] and increasing the expression of AQP5 and VIP to alleviate glandular damage [23,24]. Recent research indicates that traditional Chinese medicine may regulate immune diseases by modulating the gut microbiota [25–28]. It remains to be seen whether MDDST exerts its therapeutic effects through the regulation of the gut microbiota or the production of SCFAs. Therefore, the aim of this study is to investigate the mechanism of MDDST on SCFAs and Th17/Treg in NOD mice.

2. Materials and methods

This study was conducted in 2023 at the Animal Experiment Center of Nanjing University of Chinese Medicine, Nanjing, China.

2.1. Materials and reagents

Mouse IgG, SSA, IL-6, IL-17, IL-10 and TGF-β ELISA kits were purchased from ZCIBIO Technology Co., Ltd (Shanghai, China). Mouse-FITC-anti-CD4, Mouse-APC-anti-CD25, Mouse-PE-anti-Foxp3 and Mouse-PE-anti-IL-17A were purchased from eBioscience (San Diego, USA). Leukocyte Activation Cocktail and Transcription Factor Buffer Set were purchased from BD Pharmingen (San Diego, USA). Ampicillin was purchased from Shanghai Macklin Biotech Co., Ltd (Shanghai, China), while Vancomycin, metronidazole and neomycin were purchased from Yuanye Biotech Co., Ltd (Shanghai, China). Sodium acetate, sodium butyrate and sodium propionate were also purchased from Yuanye Biotech Co., Ltd (Shanghai, China). The purity of each compound was above 98 percent. Other reagents and solvents used were of analytical grade.

2.2. Preparation of MDDST

A mixture consisting of 20 g of dwarf lilyturf tuber, 15 g of rehmannia root, 15 g of white peony root, 10 g of peach seed and 10 g of tatarian aster root was immersed in distilled water for 30 min, followed by a boiling period of 20 min. The filtrates were concentrated using rotary evaporation, resulting in a crude drug content of 1.4 g/mL.

2.3. Chemical profiling of MDDST

The chemical composition of MDDST was characterized using UHPLC–QE-MS analysis, which was performed with the Vanquish UHPLC system (Thermo Fisher Scientific, Waltham, MA, USA) and the Q Exactive HF MS system (Thermo Fisher Scientific). The UHPLC analysis was carried out on a Waters UPLC BEH C18 column (1.7 μm, 2.1 mm × 100 mm) with an injection volume of 5 μL and a flow rate of 0.5 mL/min. The mobile phase consisted of a 0.1 percent formic acid aqueous solution and a 0.1 percent formic acid acetonitrile solution, following a multi-step linear elution gradient program. Mass spectrometry conditions for the identification of active ingredients included a mass range of 100∼1500 in each collection cycle, utilizing a heated electrospray ionization source for positive and negative ion mode detection. Retention time correction, peak identification and peak integration were performed on the

original mass spectrometry data and a custom mass spectrometry database and matching algorithms were employed to identify the substances in the results.

2.4. Animal models

The animal experiments were approved by the Experimental Animal Ethics Committee of Nanjing University of Traditional Chinese Medicine (No.202303A035). Forty-five eight-week-old female non-obese diabetes (NOD/Ltj) mice and five eight-week-old female ICR mice were obtained from the Experimental Animal Center of Nanjing University of Chinese Medicine. The ICR mice served as the control group, while the NOD mice were randomly divided into nine groups (n = 5): model group and low-, middle-, high-dose MDDST groups (L-MDDST, M-MDDST, H-MDDST: 2, 4 and 8 g/kg/d, respectively), NOD-FMT group, MDDST-FMT group and the SCFAs group (Acetate, Propionate, Butyrate group). After an adaptation period, MDDST and SCFAs were administered for 12 weeks, while the control and model mice were given an equal volume of saline. All mice were housed in a controlled environment with a temperature of 22 °C ± 2 °C, relative humidity of 55 ± 5 percent, and a 12-h light/dark cycle. They were provided with water and food ad libitum. The mice were weighed every two weeks.

2.5. Fecal microbiota transplantation (FMT)

After 4 weeks of MDDST administration, fecal samples were collected daily from mice in the model and H-MDDST groups. The feces were thoroughly homogenized and dissolved in PBS (1 mL/100 mg feces), followed by vortexing for 5 min and settling at room temperature for 15 min. The supernatant was collected for gavage administration.

Mice in the NOD-FMT and MDDST-FMT groups were administered antibiotic cocktails (vancomycin at a concentration of 0.5 mg/mL and ampicillin, metronidazole, neomycin at a concentration of 1 mg/mL) instead of drinking water for a duration of three weeks [29]. Subsequently, gavage was performed using fecal samples from the model and MDDST groups respectively. This intervention lasted for four weeks.

2.6. SCFAs intervention

After adaptive feeding, mice in the SCFAs group were administered SCFAs (acetate, propionate and butyrate were diluted with purified water to 150 mmol/L, respectively) with free access to water. This treatment lasted for 8 weeks.

2.7. Terminal water intake and spleen index

The terminal water intake (mL/g/d) was determined by calculating the average daily water consumption over the last 7 d per mouse in each experimental group (n = 5). After the mice were euthanized using cervical dislocation, spleen weight was measured. The spleen index (mg/g) was calculated as the ratio between spleen weight and mouse weight.

2.8. Serum biochemical parameter analysis

Prior to euthanizing the mouse, blood is collected, followed by centrifugation at 3000 rpm for 10 min to separate the serum. The levels of SSA, IgG, IL-6, IL-17, IL-10 and TGF-β are quantified using their respective ELISA kit protocols.

2.9. Histochemical analysis

The submandibular glands were removed from the mice after they were sacrificed. The glands were then fixed with 4 percent paraformaldehyde, dehydrated and embedded in paraffin. The tissues were cut into 5 μm thick sections and stained with HE. Histopathological changes were assessed and photographed using an optical photomicroscope (Olympus, Japan). The Chisholm-Mason grading system was used to evaluate pathological grade.

2.10. Flow cytometry

Fresh spleens were mechanically dissociated. Subsequently, red blood cells were lysed and the resulting single cell suspensions were filtered through a nylon membrane before being centrifuged at 1200 rpm for 5 min. The resultant precipitate was resuspended in RPMI1640 medium supplemented with 10 percent FBS and stimulated with leukocyte activation cocktail. The flow cytometry assay allowed for the determination of the number of Th17 cells ($CD4^+IL\text{-}17A^+$) and Treg cells ($CD4^+$ $CD25^+$ $Foxp3^+$) after the antibody staining respectively. The results were analyzed using FlowJo 10.8.1.

2.11. Gut microbiota analysis by 16S rDNA

Mouse feces were collected by gently rubbing the abdomen of the mouse. A total of 3–5 fecal pellets were collected in a sterile centrifuge tube and immediately stored at −80 °C for future use. The manufacturer's protocol was followed for DNA extraction, PCR amplification, product purification, quality inspection, library construction, high-throughput sequencing, data processing, OTU table

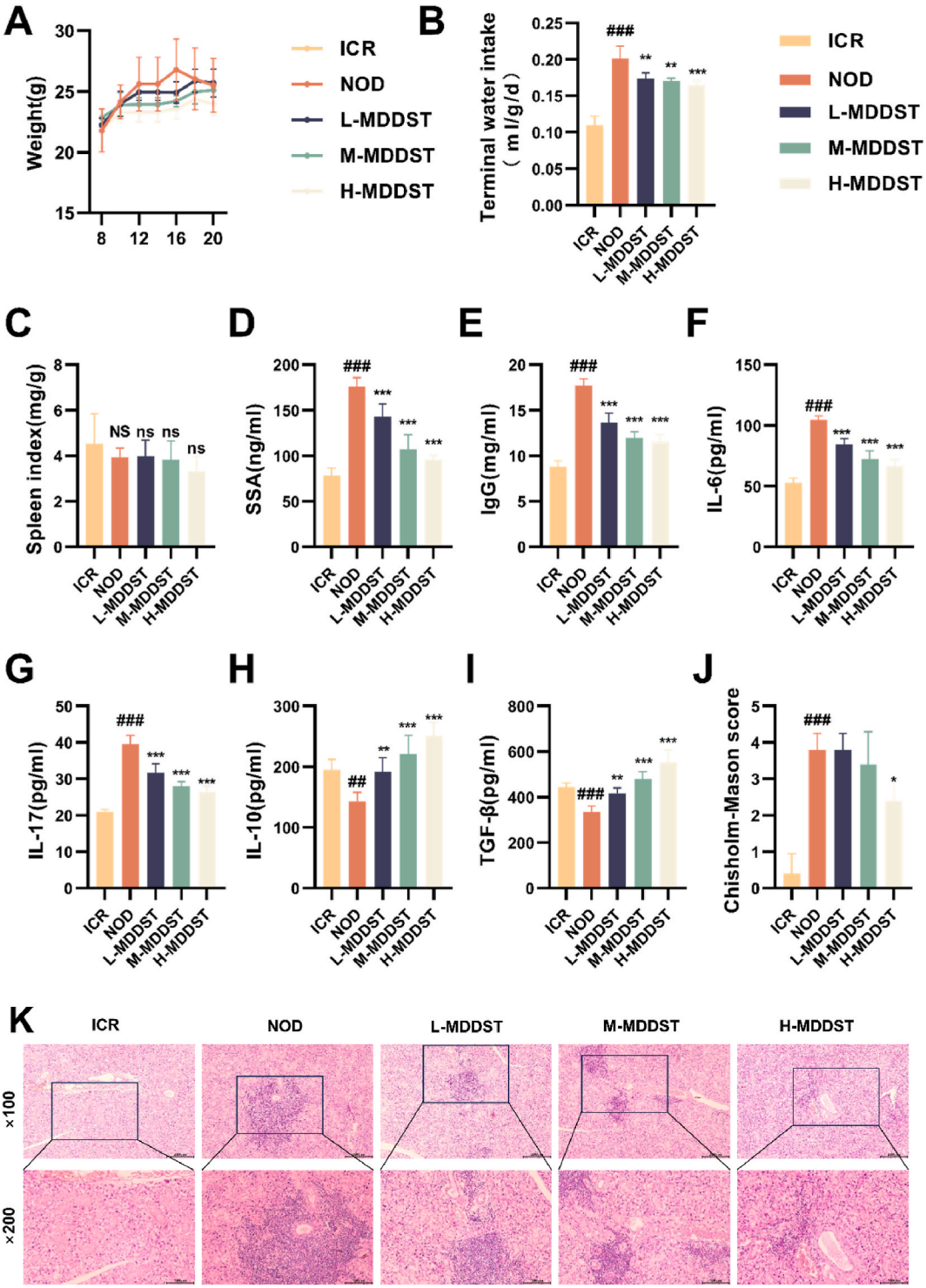

Fig. 1. MDDST treatment alleviated the symptoms of pSS in NOD mice. (A) Weight results, terminal water intake and Spleen index of each group, n = 5. (D–I) The serum levels of SSA, IgG, IL-6, IL-17, IL-10, TGF-β in mice, n = 5. (J) Chisholm-Mason score, n = 5. (K) HE staining results of submandibular gland of each group. Compared with the control group, NS represents $p > 0.05$, $^{\#}p < 0.05$, $^{\#\#}p < 0.01$, $^{\#\#\#}p < 0.001$. Compared with the model group, NS represents $p > 0.05$, $^{*}p < 0.05$, $^{**}p < 0.01$, $^{***}p < 0.001$.

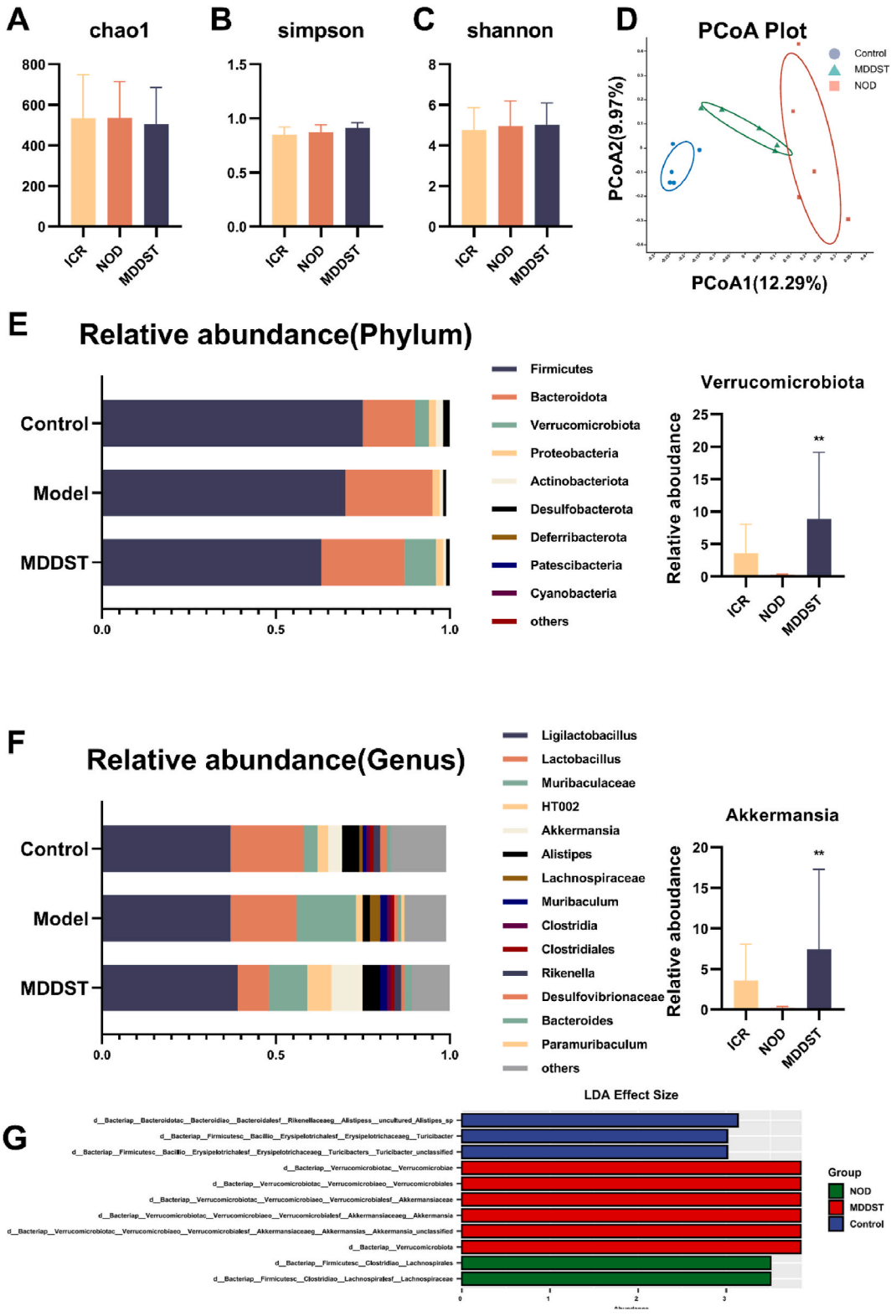

Fig. 2. MDDST regulated the gut microbiota in NOD mouse. (A–C) Chao1, Simpson and Shannon values, n = 5. (D) A Principal Coordinates Analysis (PCoA) plot based on binary-Jaccard algorithm. (E) Microbial composition of phylum level, n = 5. (F) Microbial composition of genus level, n = 5. (G) Distribution histogram of LEfSe analysis. **p < 0.01.

construction and data analysis. R 4.3.2 and Majorbio Cloud Platform were utilized for the data analysis.

2.12. Feces SCFAs analysis

Ten milligrams of mouse feces were accurately weighed, and 1 mL of 70 percent acetonitrile was added. The mixture was homogenized and centrifuged at 13,000 rpm for 10 min. A volume of 40 μL of the supernatant was transferred into a 1.5 mL centrifuge tube, followed by the addition of 5 μL of D3-hexanoic acid (10 μg/mL) as the internal standard. The mixture was vortexed for 3 min, after which 20 μL of 3 NPH and 20 μL of a 200 mM EDC · HCl-6 percent pyridine solution were added. The mixture was vortexed again for 3 min and allowed to react at 40 °C for 30 min. Subsequently, the mixture was centrifuged at 18,000 rpm for 10 min, and the supernatant was collected for analysis. Appropriate amounts of acetic acid, propionic acid, butyric acid, isobutyric acid, 2-methylbutyric acid, valeric acid, and isovaleric acid were accurately weighed, and solutions with varying gradient concentrations were prepared to establish the standard curve. Chromatographic conditions: Injection volume: 1 μL- Chromatography column: TG-5MS capillary column (0.25 mm·30 m·0.25 μm, Thermo, USA)- Gradient heating program: 0–2 min: 50 °C - 2–4 min: 50–70 °C - 4–9 min: 70–85 °C - 9–14 min: 85–110 °C - 14–20 min: 110–290 °C - 20–28 min: 290°C- Split mode with a split ratio of 20:1Ionization method: Electron bombardment ion source (EI) with an ionization energy of 70 eV- Ion transport temperature: 290°C- Ion source temperature: 230°C- Mass spectrometry scanning range: 30–600 m/z- Scanning method: Full scan- Carrier gas: High-purity helium (purity>99.999 percent)- Airflow speed: 1.2 mL/min.

2.13. Statistical analysis

The data analysis was conducted using GraphPad Prism 9.5.1 software. The mean ± SD was utilized to present the data. The comparison between the two groups was evaluated through an independent sample *t*-test. Differences among multiple groups were examined using one-way analysis of variance (ANOVA) followed by the Tukey post-hoc test. The Kruskal-Wallis rank-sum test was applied to identify species with significant abundance differences. GraphPad Prism was also employed for data visualization. A p-value less than 0.05 was considered statistically significant in the data analysis findings.

3. Results

3.1. MDDST treatment alleviated the symptoms of pSS in NOD mouse

The representative chromatograms of MDDST extracted solution are illustrated in Fig. S1. The UHPLC-MS analysis results showed that the components were identified and detected based on their retention times, as detailed in Table S2. Specifically, there were 2 constituents attributed to Maidong (dwarf lilyturf tuber), 7 constituents attributed to Dihuang (rehmannia root), 6 constituents attributed to Baishao (white peony root), 4 constituents attributed to Taoren (peach seed) and 11 constituents attributed to Ziwan (tatarian aster root).

The therapeutic effectiveness of MDDST in pSS was evaluated by administering varying doses of MDDST via oral gavage to NOD mice, and the results are illustrated in Fig. 1. Compared to the control group, NOD mice demonstrated a significant disease status, as indicated by increased water intake, elevated levels of SSA, heightened IgG levels. After the administration of MDDST, these indicators showed marked improvement (Fig. 1B–E). Subsequently, we assessed the levels of inflammatory factors in the serum of NOD mice. Relative to the control group, serum levels of IL-6 and IL-17 were significantly elevated in NOD mice, while IL-10 and TGF-β levels were markedly decreased, indicating a pronounced inflammatory state. These inflammatory markers improved subsequent to MDDST treatment (Fig. 1F–I). Furthermore, pathological examination of the submandibular gland tissue sections from the control group of ICR mice revealed smooth edges of glandular ducts, abundant acini and an absence of significant inflammatory infiltration. In contrast, NOD mice demonstrated atrophy of glandular ducts, a reduction in acini, infiltration and aggregation of inflammatory cells (Fig. 1K). Importantly, MDDST treatment effectively ameliorated these pathological alterations, as evidenced by the Chisholm-Mason histopathological score (Fig. 1J).

3.2. MDDST changed the ratio of Th17 and Treg cells in spleen and regulated the gut microbiota in NOD mouse

To evaluate the effect of MDDST on Th17/Treg immune cells, we performed flow cytometry on spleen cells from NOD mice, with results presented in Fig. S2. The proportion of Th17 cells in NOD mice was higher compared to the ICR control group. However, after MDDST intervention, a significant decrease in the proportion of Th17 cells was observed. Conversely, the proportion of Treg cells in NOD mice was lower than that in the control group, but it increased significantly after MDDST treatment. These findings suggest that the immune balance of Th17/Treg is disrupted in NOD mice, and that MDDST can effectively regulate the populations of Th17 and Treg cells, thereby promoting the restoration of Th17/Treg immune balance.

The structure of gut microbiota in mice was analyzed using 16S rDNA (Fig. 2). The results indicated that there were no significant differences in the Chao1, Simpson and Shannon indexes (Fig. 2A–C). The PCoA plot demonstrated that the gut microbiota in the MDDST group was more similar to the control group than the model group (Fig. 2D). Further examination of the gut microbiota composition revealed a significant increase in the relative abundance of Verrucomicrobia at the phylum level after MDDST intervention. Additionally, at the genus level, MDDST administration significantly increased the relative abundance of Akkermansia (Fig. 2E and F). Linear discriminant analysis Effect Size (LEfSe) analysis identified several microbiomes that showed significant

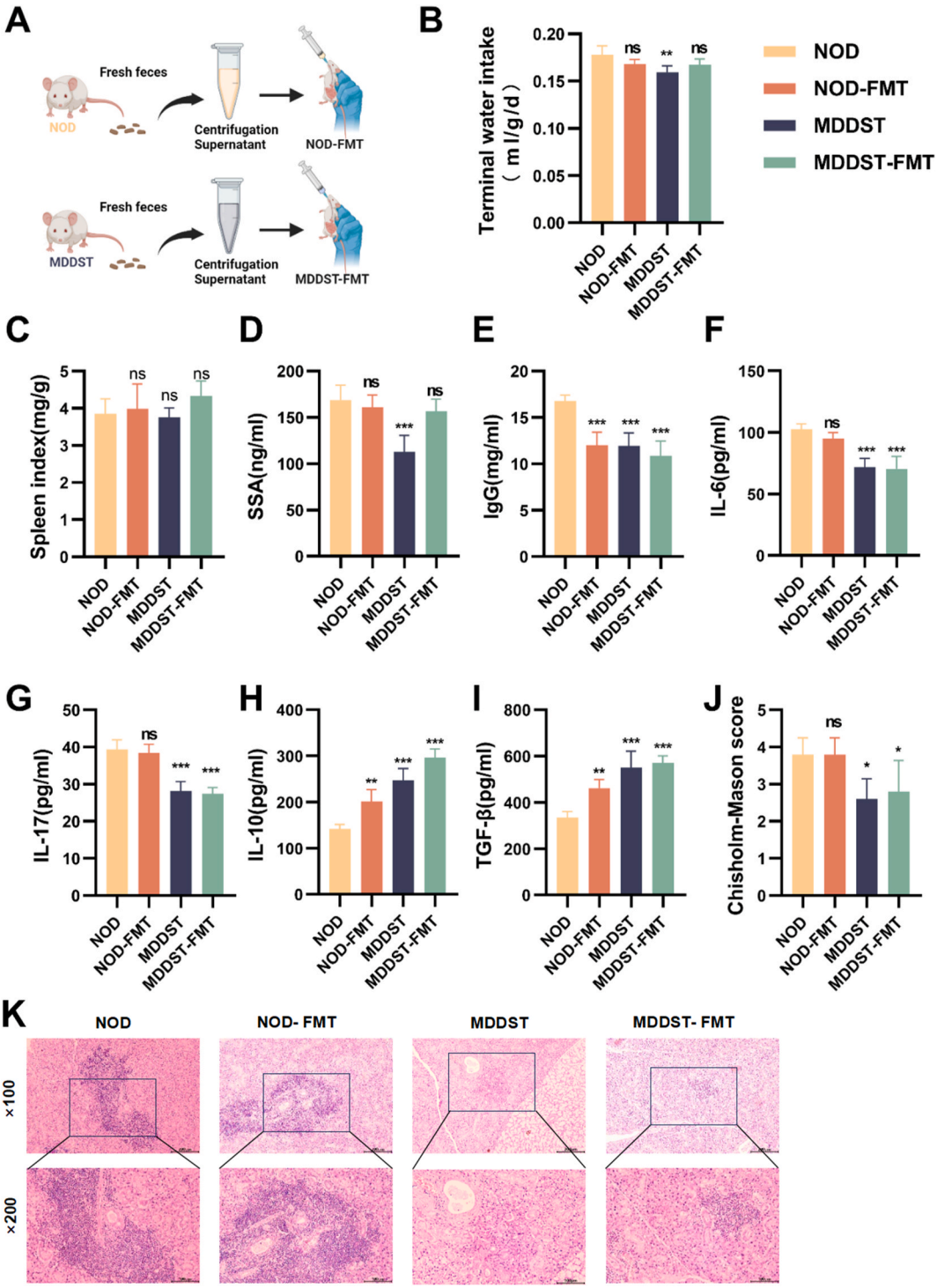

Fig. 3. Fecal microbiota transplantation similarly alleviated the symptoms of pSS. (A) Study design of FMT on pSS development in NOD mouse. (B–C) Terminal water intake and spleen index of each group, n = 5. (D–I) The serum levels of SSA, IgG, IL-6, IL-17, IL-10, TGF-β in mice, n = 5. (J) Chisholm-Mason score, n = 5. (K) HE staining results of submandibular gland of each group. Compared with the control group, NS represents $p > 0.05$, $^{\#}p < 0.05$, $^{\#\#}p < 0.01$, $^{\#\#\#}p < 0.001$. Compared with the model group, NS represents $p > 0.05$, $^{*}p < 0.05$, $^{**}p < 0.01$, $^{***}p < 0.001$.

differences, including Alistipess, Turicibacter, Lachnospiraceae and Akkermansia. Therefore, MDDST had a discernible impact on a small fraction of the gut microbiota in NOD mice.

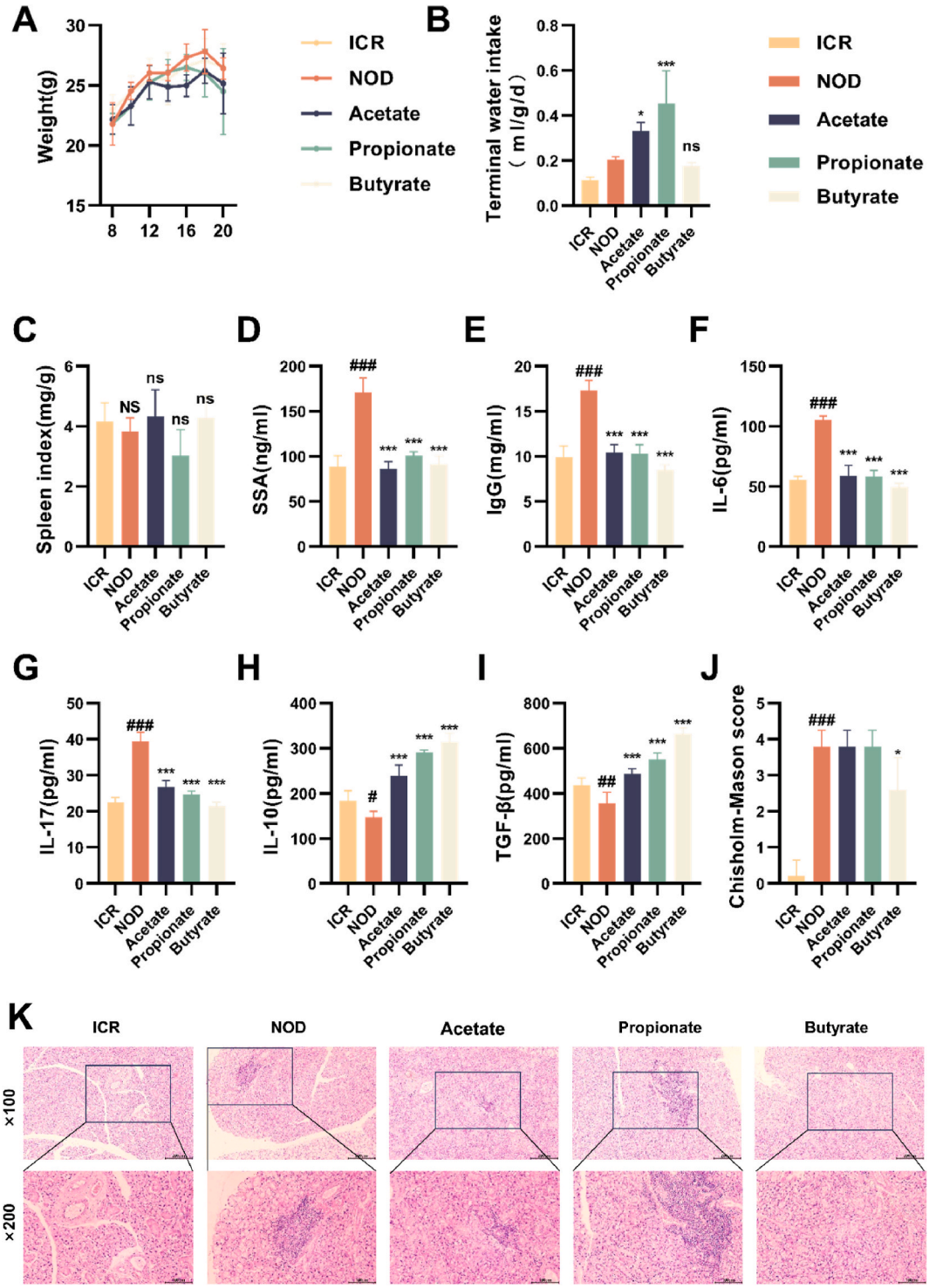

Fig. 4. Effects of SCFAs in NOD mouse. (A–C) Weight, terminal water intake and spleen index of each group, n = 5. (D–I) The serum levels of SSA, IgG, IL-6, IL-17, IL-10, TGF-β in mice, n = 5. (J) Chisholm-Mason score, n = 5. (K) He staining results of submandibular gland of each group. Compared with the control group, NS represents $p > 0.05$, $^{\#}p < 0.05$, $^{\#\#}p < 0.01$, $^{\#\#\#}p < 0.001$. Compared with the model group, NS represents $p > 0.05$, $^{*}p < 0.05$, $^{**}p < 0.01$, $^{***}p < 0.001$.

3.3. MDDST modulated the metabolites of gut microbiota in NOD mouse and fecal microbiota transplantation similarly alleviated the symptoms of pSS

The content of SCFAs in the feces of NOD mice was analyzed using targeted metabolomics (Fig. S3). Compared to the control group, the propionate levels in the intestines of NOD mice decreased (Fig. S3B; $p < 0.05$), while acetate and butyrate showed a decreasing trend. There was no significant difference in the levels of isobutyrate acid, 2-methyl-butyrate, valerate and isovalerate. However, after the intervention of MDDST, there was a significant increase in acetate and butyrate (Figs. S3A and S3C; $p < 0.05$) and the propionate also showed a significant recovery. No significant difference was observed in the rest of the SCFAs. These results indicate that MDDST increased the gut SCFAs level in NOD mouse.

To further evaluate the association between the gut microbiota and MDDST, the fecal microbiota of model and H-MDDST groups was transplanted to microbiota depleted NOD mice (Fig. 3A). Compared to the NOD mouse, NOD-FMT group showed similar pSS disease symptoms, including increased water intake, serum autoantibodies, inflammatory cytokines (Fig. 3B–G) and histopathological findings (Fig. 3J and K). Compared to the NOD-FMT group, MDDST-FMT group showed improvement in disease status, similar to MDDST group (Fig. 3). Interestingly, despite the transplantation of feces from mice in a diseased state, the levels of IgG, IL-10 and TGF-β exhibited contrasting results. This observation may be attributed to the absence of pathogenic bacteria during the modeling process. Consequently, MDDST-FMT demonstrated a modest alleviation of symptoms in NOD mice. The potential amelioration of pSS by MDDST could be partially mediated through modulation of gut microbiota.

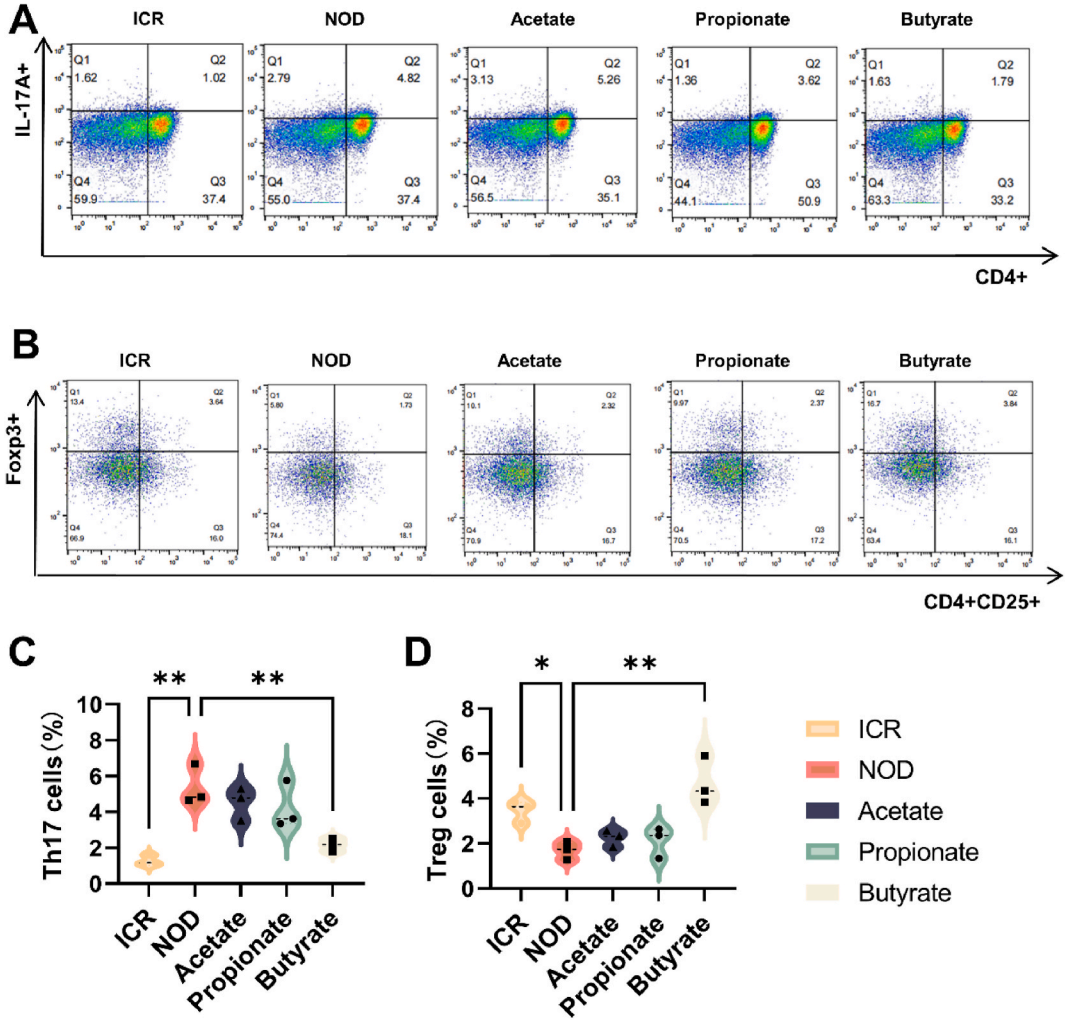

Fig. 5. Butyrate regulated the Th17/Treg immune balance in NOD mice. (A–B) Proportion of $CD4^+IL\text{-}17A^+$Th17 cells in spleen. (C–D) Proportion of $CD4^+CD25^+Foxp3^+$Treg cells in spleen. *$p < 0.05$, **$p < 0.01$.

3.4. Effects of SCFAs in NOD mouse

To further investigate the relationship between MDDST and SCFAs, we selected acetate, propionate and butyrate as intervention media. Comparing to the model group, the acetate group and propionate group showed an increase in terminal water intake (Fig. 4B; $p < 0.05$). Treatment with acetate, propionate and butyrate resulted in a significant decrease in serum levels of SSA, IgG, IL-6 and IL-17 (Fig. 4D–G; $p < 0.05$), as well as an increase in serum levels of IL-10 and TGF-β (Fig. 4H and I; $p < 0.05$). Histopathological analysis revealed that only the butyrate group showed a protective effect (Fig. 4J and K; $p < 0.05$). In summary, SCFAs treatment significantly improved pSS symptoms and serum indicators and butyrate had a protective effect on submandibular gland.

3.5. Butyrate regulated the Th17/Treg immune balance in NOD mice

The effect of SCFA administration on Th17 and Treg immune cells was evaluated using flow cytometry, with results presented in Fig. 5. The proportion of Th17 cells in NOD mice was found to be higher compared to the ICR control group. However, following butyrate intervention, a significant decrease in the proportion of Th17 cells was observed (Fig. 5A and C). In contrast, neither the acetate nor propionate groups exhibited any improvement. Conversely, the proportion of Treg cells in NOD mice significantly increased after butyrate treatment (Fig. 5B and D). These findings suggest that butyrate plays a role in regulating the Th17/Treg immune balance in NOD mice.

4. Discussion

Primary Sjogren's syndrome is a chronic autoimmune disease, with current treatment options primarily focusing on suppressing abnormal immune responses. The International pSS Management Guidelines recommend medication for both local and systemic treatments. However, conventional synthetic disease-modifying antirheumatic drugs (DMARDs) and glucocorticoids have limitations in effectively managing symptoms and often come with numerous side effects. Traditional Chinese medicine, used as a complementary treatment for pSS, is characterized by its multiple components, targets, and pathways, and has shown promising results in China. Therefore, investigating the effective ingredients and mechanisms of MDDST treatment holds translational value in the development of clinical alternative therapies for pSS.

In this study, the therapeutic effect of MDDST was evaluated by observing the general state of NOD mice, examining HE staining pathological results, measuring serum antibody and inflammatory factor levels. These results demonstrated that the model mice exhibited typical manifestations of Sjogren's syndrome, such as increased water intake, hair loss and significant lymph infiltration in the submandibular gland. Following the intervention of MDDST, there was a significant improvement in pathological damage, serum antibodies and inflammatory factors. These findings are consistent with previous research. Thus, the results indicate that the pSS model was successfully replicated in NOD mice and that MDDST had a definite effect on this model.

The imbalance between Th17 and Treg cells is known to play a crucial role in the development of pSS disease. During the active phase of pSS, there is an increase in Th17 cells and pro-inflammatory cytokines IL-6 and IL-17, while Treg cells and anti-inflammatory cytokines IL-10 and TGF-β decrease. This immune imbalance leads to immune disorders and exacerbates the inflammatory reaction. The findings of this study demonstrate that MDDST can effectively inhibit Th17 cells, increase the relative number of Treg cells and promote the immune balance between Th17 and Treg cells. So, MDDST has the potential to reduce the number of Th17 cells and increase the number of Treg cells.

Gut microbiota, the largest symbiotic microbial community in the human body, has been extensively studied for its role in autoimmune diseases [30–33]. Previous research has shown a correlation between microbiota imbalance and disease activity of pSS patients [34,35]. The analysis of 16S rDNA revealed that in the NOD group mice, there was a decrease in the relative abundance of Verrucomimicrobia at the phylum level and Akkermansia at the genus level. However, after the administration of MDDST, the decrease in relative abundance was reversed. Akkermansia is known to produce propionate and butyrate, which play a role in regulating intestinal barrier function, antimicrobial peptide production, immune regulation, the differentiation of Treg cells and the secretion of IL-10 [36]. Therefore, Akkermansia is a probiotic with significant research potential. These findings highlight the differences in the microbiota between the ICR mouse and NOD mouse, and demonstrate that the intervention of MDDST had a discernible impact on a small fraction of the gut microbiota in NOD mice. To investigate whether MDDST can exert a therapeutic effect on NOD mice by regulating the gut microbiota, we conducted a fecal bacteria transplantation experiment. We transplanted the intestinal microbiota from the model group and MDDST group into NOD mice that had previously been depleted of flora. When comparing the NOD-FMT group to the MDDST-FMT group, we observed decreased levels of IL-6 and IL-17, as well as increased levels of IL-10 and TGF-β. Additionally, the pathological score of the submandibular gland was reduced. These findings suggest that FMT can partially improve the disease status of NOD mice and that MDDST may have a partial effect on improving Sjogren's syndrome through the modulation of gut microbiota.

Short chain fatty acids are important intestinal metabolites that play a role in various biological processes such as energy metabolism, cell differentiation, immune regulation and enhancing the function of the intestinal barrier. They have been the focus of research in inflammatory autoimmune diseases. Clinical studies have found a reduction in butyrate-producing bacteria in the gut of pSS patients, which is associated with disease severity [35]. Similar results have been observed in animal models of pSS [37] and supplementation with SCFAs can lead to clinical remission [10,38]. Therefore, SCFAs have the potential to be used in the treatment of pSS. To investigate the correlation between MDDST and SCFAs, the levels of fecal SCFAs were measured using targeted metabonomics in each group. The results showed that MDDST increased the gut SCFAs level in NOD mouse. Further verification of the effects of

acetate, propionate and butyrate on NOD mice revealed that SCFAs treatment significantly improved pSS symptoms and serum indicators and butyrate has a positive effect pathological injury and regulate Th17/Treg immune balance.

The findings of this study suggest that MDDST effectively improves the disease status of pSS model mice. This improvement may be attributed to the modulation of gut microbiota, SCFAs and the balance between Th17 and Treg cells (Fig. 6). These results provide experimental evidence for the application of MDDST in pSS treatment. Moreover, this study emphasizes the significant role played by gut microbiota in the underlying pathological mechanism of pSS. In addition, these research results also provide ideas for future research directions, such as developing new probiotic assisted therapy methods, developing therapeutic drugs based on SCFAs, and evaluating the dose-response relationship of SCFAs. In the future, we will strive to further clarify the specific regulatory mechanisms of MDDST, in order to provide a research foundation for the clinical translational application of MDDST.

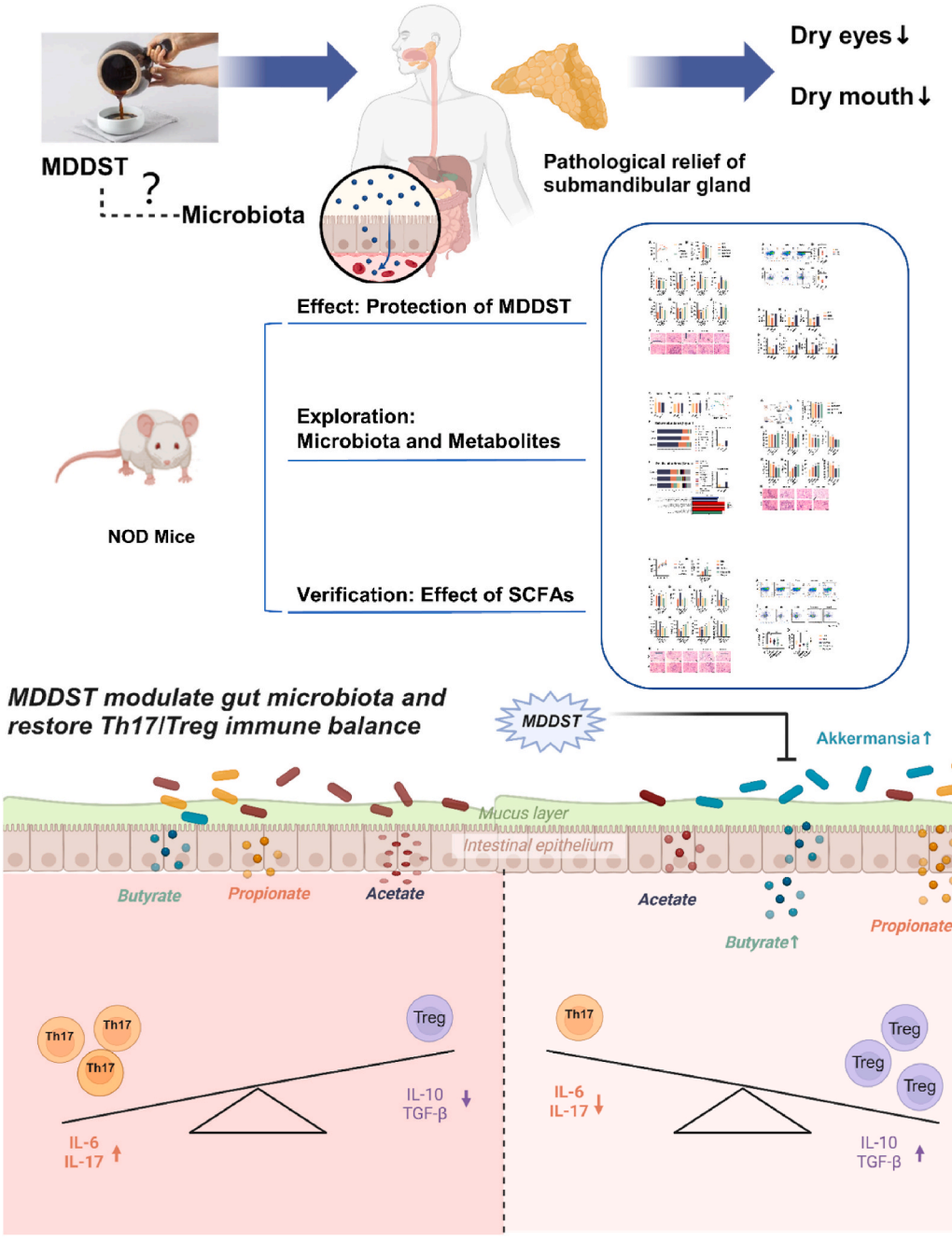

Fig. 6. MDDST plays a role in reshaping the Th17/Treg immune balance and alleviating the progression of Sjogren's syndrome by regulating gut microbiota and short chain fatty acids.

This study remains several limitations. Variables such as diet, living conditions and experimental procedures may have an impact on the results obtained. Additionally, further investigation, such as the analysis of fecal microbiome and metabolomics, is imperative to comprehensively elucidate the precise mechanism through which MDDST impacts gut microbiota and SCFAs. Furthermore, additional studies are necessary to explore the use of MDDST in pSS patients, including an assessment of its safety and effectiveness. These limitations necessitate addressing in future research.

5. Conclusion

In conclusion, MDDST effectively mitigates submandibular gland injury and restores the Th17/Treg immune balance in NOD mice. The exploration of underlying mechanisms elucidates the roles of gut microbiota and SCFAs in the therapeutic effects of MDDST. The results of this study provide support the therapeutic application of MDDST and present a novel treatment option for patients with pSS. However, it is important to note that gut microbiota and SCFAs can be influenced by various factors, including diet, environment and treatment, and there are notable differences between human and animal models, which may affect the interpretation of experimental results. Future studies should focus on specific bacterial genera and therapeutic mechanisms through clinical investigations.

Data availability

The data are available from the corresponding author upon reasonable request.

Ethics statement

All animal experiments were conducted in accordance with institutional, national, or international guidelines and were approved by the Experimental Animal Ethics Committee of Nanjing University of Traditional Chinese Medicine (No.202303A035).

Funding

This work was supported by the National Natural Science Foundation of China (Grant Number 82274454).

Additional information

No additional information is available for this paper.

CRediT authorship contribution statement

Yue Zhang: Writing – original draft, Validation, Methodology, Investigation, Data curation, Conceptualization. **Yunxia Wu:** Visualization, Validation, Software, Methodology, Investigation, Data curation. **Yin Guan:** Validation, Methodology, Investigation. **Yun Lu:** Validation, Methodology, Investigation. **Wen Zhu:** Writing – review & editing, Supervision, Methodology. **Fan Ping:** Supervision, Project administration, Methodology. **Yue Wang:** Supervision, Resources, Methodology, Funding acquisition, Conceptualization.

Declaration of competing interest

The authors declare that they have no known competing financial interests or personal relationships that could have appeared to influence the work reported in this paper.

Abbreviations

ANOVA	One-way analysis of variance
FMT	fecal microbiota transplantation
HE	Hematoxylin and Eosin
IgG	Immunoglobulin G
IL-10	Interleukin- 10
IL-17	Interleukin- 17
IL-6	Interleukin- 6
MDDST	Maidong Dishao Decoction
NOD	Non-Obese Diabetes
OUT	Operational taxonomic units
pSS	Primary Sjogren's syndrome
SCFAs	Short chain fatty acids
TCM	Traditional Chinese medicine;
TGF-β	Transforming growth factor beta

Th17 T helper cell 17
Treg regulatory T cell

Appendix A. Supplementary data

Supplementary data to this article can be found online at https://doi.org/10.1016/j.heliyon.2024.e38421.

References

[1] G.E. Thorlacius, A. Bjork, M. Wahren-Herlenius, Genetics and epigenetics of primary Sjogren syndrome: implications for future therapies, Nat. Rev. Rheumatol. 19 (5) (2023) 288–306, https://doi.org/10.1038/s41584-023-00932-6.

[2] J. Tarn, D. Lendrem, P. McMeekin, C. Lendrem, B. Hargreaves, W.-F. Ng, Primary Sjogren's syndrome: longitudinal real-world, observational data on health-related quality of life, J. Intern. Med. 291 (6) (2022) 849–855, https://doi.org/10.1111/joim.13451.

[3] N. Conrad, S. Misra, J.Y. Verbakel, G. Verbeke, G. Molenberghs, P.N. Taylor, J. Mason, N. Sattar, J.J. V McMurray, I.B. McInnes, K. Khunti, G. Cambridge, Incidence, prevalence, and co-occurrence of autoimmune disorders over time and by age, sex, and socioeconomic status: a population-based cohort study of 22 million individuals in the UK, Lancet 401 (10391) (2023) 1878–1890, https://doi.org/10.1016/s0140-6736(23)00457-9.

[4] C.M. Trujillo-Vargas, L. Schaefer, J. Alam, S.C. Pflugfelder, R.A. Britton, C.S. de Paiva, The gut-eye-lacrimal gland-microbiome axis in Sjogren Syndrome, Ocul. Surf. 18 (2) (2020) 335–344, https://doi.org/10.1016/j.jtos.2019.10.006.

[5] S. Liu, X. Men, Y. Guo, W. Cai, R. Wu, R. Gao, W. Zhong, H. Guo, H. Ruan, S. Chou, J. Mai, S. Ping, C. Jiang, H. Zhou, X. Mou, W. Zhao, Z. Lu, Gut microbes exacerbate systemic inflammation and behavior disorders in neurologic disease CADASIL, Microbiome 11 (1) (2023) 202, https://doi.org/10.1186/s40168-023-01638-3.

[6] T. Mukherjee, N. Kumar, M. Chawla, D.J. Philpott, S. Basak, The NF-κB signaling system in the immunopathogenesis of inflammatory bowel disease, Sci. Signal. 17 (818) (2024) eadh1641, https://doi.org/10.1126/scisignal.adh1641.

[7] J. Wang, W.-D. Chen, Y.-D. Wang, The relationship between gut microbiota and inflammatory diseases: the role of macrophages, Front. Microbiol. 11 (2020) 1065, https://doi.org/10.3389/fmicb.2020.01065.

[8] J. Goc, M. Lv, N.J. Bessman, A.-L. Flamar, S. Sahota, H. Suzuki, F. Teng, G.G. Putzel, G. Eberl, D.R. Withers, J.C. Arthur, M.A. Shah, G.F. Sonnenberg, J.R.I.L. C. Bank, Dysregulation of ILC3s unleashes progression and immunotherapy resistance in colon cancer, Cell 184 (19) (2021) 5015–5030, https://doi.org/10.1016/j.cell.2021.07.029.

[9] Y. Harada, T. Sujino, K. Miyamoto, E. Nomura, Y. Yoshimatsu, S. Tanemoto, S. Umeda, K. Ono, Y. Mikami, N. Nakamoto, K. Takabayashi, N. Hosoe, H. Ogata, T. Ikenoue, A. Hirao, Y. Kubota, T. Kanai, Intracellular metabolic adaptation of intraepithelial CD4+CD8αα+ T lymphocytes, iScience 25 (4) (2022) 104021, https://doi.org/10.1016/j.isci.2022.104021.

[10] D.S. Kim, J.S. Woo, H.-K. Min, J.-W. Choi, J.H. Moon, M.-J. Park, S.-K. Kwok, S.-H. Park, M.-L. Cho, Short-chain fatty acid butyrate induces IL-10-producing B cells by regulating circadian-clock-related genes to ameliorate Sjogren's syndrome, J. Autoimmun. 119 (2021) 102611, https://doi.org/10.1016/j.jaut.2021.102611.

[11] X. Liang, C.-S. Liu, X.-H. Wei, T. Xia, F.-L. Chen, Q.-F. Tang, M.-Y. Ren, X.-M. Tan, Mahuang Fuzi Xixin decoction ameliorates allergic rhinitis in rats by regulating the gut microbiota and Th17/Treg balance, J Immunol Res 2020 (2020) 6841078, https://doi.org/10.1155/2020/6841078.

[12] S. Luo, R. Wen, Q. Wang, Z. Zhao, F. Nong, Y. Fu, S. Huan, J. Chen, L. Zhou, X. Luo, Rhubarb Peony Decoction ameliorates ulcerative colitis in mice by regulating gut microbiota to restoring Th17/Treg balance, J. Ethnopharmacol. 231 (2019) 39–49, https://doi.org/10.1016/j.jep.2018.08.033.

[13] S. Ma, J. Yeom, Y.-H. Lim, Specific activation of hypoxia-inducible factor-2α by propionate metabolism via a β-oxidation-like pathway stimulates MUC2 production in intestinal goblet cells, Biomed. Pharmacother. 155 (2022) 113672, https://doi.org/10.1016/j.biopha.2022.113672.

[14] A. Duscha, B. Gisevius, S. Hirschberg, N. Yissachar, G.I. Stangl, E. Dawin, V. Bader, S. Haase, J. Kaisler, C. David, R. Schneider, R. Troisi, D. Zent, T. Hegelmaier, N. Dokalis, S. Gerstein, S. Del Mare-Roumani, S. Amidror, O. Staszewski, G. Poschmann, K. Stuehler, F. Hirche, A. Balogh, S. Kempa, P. Traeger, M.M. Zaiss, J. B. Holm, M.G. Massa, H.B. Nielsen, A. Faissner, C. Lukas, S.G. Gatermann, M. Scholz, H. Przuntek, M. Prinz, S.K. Forslund, K.F. Winklhofer, D.N. Mueller, R. A. Linker, R. Gold, A. Haghikia, Propionic acid shapes the multiple sclerosis disease course by an immunomodulatory mechanism, Cell 180 (6) (2020) 1067–1080, https://doi.org/10.1016/j.cell.2020.02.035.

[15] J. Moleon, C. Gonzalez-Correa, S. Minano, I. Robles-Vera, N. de la Visitacion, A.M. Barranco, M. Gomez-Guzman, M. Sanchez, P. Riesco, E. Guerra-Hernandez, M. Toral, M. Romero, J. Duarte, Protective effect of microbiota-derived short chain fatty acids on vascular dysfunction in mice with systemic lupus erythematosus induced by toll like receptor 7 activation, Pharmacol. Res. 198 (2023) 106997, https://doi.org/10.1016/j.phrs.2023.106997.

[16] N. Arpaia, C. Campbell, X. Fan, S. Dikiy, J. van der Veeken, P. deRoos, H. Liu, J.R. Cross, K. Pfeffer, P.J. Coffer, A.Y. Rudensky, Metabolites produced by commensal bacteria promote peripheral regulatory T-cell generation, Nature 504 (7480) (2013) 451–455, https://doi.org/10.1038/nature12726.

[17] H. Bartolomaeus, A. Balogh, M. Yakoub, S. Homann, L. Marko, S. Hoeges, D. Tsvetkov, A. Krannich, S. Wundersitz, E.G. Avery, N. Haase, K. Kraeker, L. Hering, M. Maase, K. Kusche-Vihrog, M. Grandoch, J. Fielitz, S. Kempa, M. Gollasch, Z. Zhumadilov, S. Kozhakhmetov, A. Kushugulova, K.-U. Eckardt, R. Dechend, L. C. Rump, S.K. Forslund, D.N. Mueller, J. Stegbauer, N. Wilck, Short-chain fatty acid propionate protects from hypertensive cardiovascular damage, Circulation 139 (11) (2019) 1407–1421, https://doi.org/10.1161/circulationaha.118.036652.

[18] J. Park, M. Kim, S.G. Kang, A.H. Jannasch, B. Cooper, J. Patterson, C.H. Kim, Short-chain fatty acids induce both effector and regulatory T cells by suppression of histone deacetylases and regulation of the mTOR-S6K pathway, Mucosal Immunol. 8 (1) (2015) 80–93, https://doi.org/10.1038/mi.2014.44.

[19] K. Zhang, Y. Wang, Treating Sjogren's syndrome by Maidongdishao decoction, Jilin Journal of Chinese Medicine 36 (4) (2016) 430–432, https://doi.org/10.13463/j.cnki.jlzyy.2016.04.033.

[20] T. Yan, Y. Wang, Clinical Observation on the Treatment of 20 Cases of Sjogren's Syndrome with Maidong Di Shao Tang, vol. 20, Journal of Nanjing University of Traditional Chinese Medicine, 2008, pp. 63–65.

[21] Y. Pan, G. Ma, J. Zhang, Y. Wang, Professor Wang Yue's experience in treating primary Sjogren's syndrome by combined treatment of lung and intestine, Asia-Pacific Traditional Medicine 20 (1) (2024) 105–109. https://kns.cnki.net/kcms/detail/42.1727.R.20230926.0923.004.html.

[22] R. Lin, D. Hao, Y. Dong, Y. Wang, Catalpol ameliorates Sjogren's Syndrome by modulating interplay of T and B cells, Biomed. Pharmacother. 123 (2020) 109806, https://doi.org/10.1016/j.biopha.2019.109806.

[23] C. Li, Y. Wang, L. Sun, T. Yan, Y. Tao, S. Wu, Protection of Ophiopoon japonicus polysaccharides on submandibular glands in NOD mice, Chinese Journal of Immunology 30 (2014) 198–201.

[24] Y. Tao, C. Li, Y. Wang, L. Sun, T. Yan, W.U. Sulin, Effects of Ophiopogon japonicus on expression of NOD mice submandibular gland AQP5 and VIPmRNA, Lishizhen Medicine and Materia Medica Research 25 (2014) 2072–2074.

[25] Y. Gu, X. Cui, J. Jiang, Y. Zhang, M. Liu, S. Cheng, Y. Li, L. ling Liu, R. Liao, P. Zhao, W. Jin, Y. Jia, J. Wang, F. Zhou, Dingxin recipe III ameliorates hyperlipidemia injury in SD rats by improving the gut barrier, particularly the SCFAs/GPR43 pathway, J. Ethnopharmacol. 312 (2023) 116483, https://doi.org/10.1016/j.jep.2023.116483.

[26] X. Wang, H. Long, M. Chen, Z. Zhou, Q. Wu, S. Xu, G. Li, Z. Lu, Modified Baihu decoction therapeutically remodels gut microbiota to inhibit acute gouty arthritis, Front. Physiol. 13 (2022) 1023453, https://doi.org/10.3389/fphys.2022.1023453.

[27] Q. Xu, Y. Yao, Y. Liu, J. Zhang, L. Mao, The mechanism of traditional medicine in alleviating ulcerative colitis: regulating intestinal barrier function, Front. Pharmacol. 14 (2023) 1228969, https://doi.org/10.3389/fphar.2023.1228969.
[28] C. Ye, Z. han Gao, Z. Bie, K. Chen, F. guo Lu, K. Wei, MXSGD alleviates CsA-induced hypoimmunity lung injury by regulating microflora metabolism, Front. Immunol. 14 (2024) 1298416, https://doi.org/10.3389/fimmu.2023.1298416.
[29] S.C. Bokoliya, Y. Dorsett, H. Panier, Y.J. Zhou, Procedures for fecal microbiota transplantation in Murine microbiome studies, Front. Cell. Infect. Microbiol. 11 (2021) 711055, https://doi.org/10.3389/fcimb.2021.711055.
[30] D. Azzouz, Z. Chen, P.M. Izmirly, L.A. Chen, Z. Li, C. Zhang, D. Mieles, K. Trujillo, A. Heguy, A. Pironti, G.G. Putzel, D. Schwudke, D. Fenyo, J.P. Buyon, A. V Alekseyenko, N. Gisch, G.J. Silverman, Longitudinal gut microbiome analyses and blooms of pathogenic strains during lupus disease flares, Ann. Rheum. Dis. 82 (10) (2023) 1315–1327, https://doi.org/10.1136/ard-2023-223929.
[31] K.M. Schneider, M. Kummen, P.J. Trivedi, J.R. Hov, Role of microbiome in autoimmune liver diseases, Hepatology 2023 (2023), https://doi.org/10.1097/hep.0000000000000506 hep.0000000000000506.
[32] T. Shao, R. Hsu, D.L. Rafizadeh, L. Wang, C.L. Bowlus, N. Kumar, J. Mishra, S. Timilsina, W.M. Ridgway, M.E. Gershwin, A.A. Ansari, Z. Shuai, P.S.C. Leung, The gut ecosystem and immune tolerance, J. Autoimmun. 141 (2023) 103114, https://doi.org/10.1016/j.jaut.2023.103114.
[33] K.N.S. Thompson, K.S.E. Bonham, N.E.J. Ilott, G.J. Britton, P.J. Colmenero, S.J.J. Bullers, L.J. McIver, S.H. Ma, L.H. Nguyen, A. Filer, I. Brough, C. Pearson, C. Moussa, V.H. Kumar, L.H.A. Lam, M.A. Jackson, A. Pawluk, S.R. Kiriakidis, P.C. Taylor, L.R.P. Wedderburn, B.R. Marsden, S.P.J. Young, D.R.G. Littman, J. J. Faith, A.G. Pratt, P. Bowness, K. Raza, F. Powrie, C. Huttenhower, M. Inflammatory Arthritis, Alterations in the gut microbiome implicate key taxa and metabolic pathways across inflammatory arthritis phenotypes, Sci. Transl. Med. 15 (706) (2023) eabn4722, https://doi.org/10.1126/scitranslmed.abn4722.
[34] T. Mandl, J. Marsal, P. Olsson, B. Ohlsson, K. Andreasson, Severe intestinal dysbiosis is prevalent in primary Sjogren's syndrome and is associated with systemic disease activity, Arthritis Res. Ther. 19 (1) (2017) 237, https://doi.org/10.1186/s13075-017-1446-2.
[35] X. Xin, Q. Wang, J. Qing, W. Song, Y. Gui, X. Li, Y. Li, Th17 cells in primary Sjogren's syndrome negatively correlate with increased Roseburia and Coprococcus, Front. Immunol. 13 (2022) 974648, https://doi.org/10.3389/fimmu.2022.974648.
[36] P.D. Cani, C. Depommier, M. Derrien, A. Everard, W.M. de Vos, Akkermansia muciniphila: paradigm for next-generation beneficial microorganisms, Nat. Rev. Gastroenterol. Hepatol. 19 (10) (2022) 625–637, https://doi.org/10.1038/s41575-022-00631-9.
[37] R. Nagatomo, H. Kaneko, S. Kamatsuki, M. Ichimura-Shimizu, N. Ishimaru, K. Tsuneyama, K. Inoue, Short-chain fatty acids profiling in biological samples from a mouse model of Sjogrens syndrome based on derivatized LC-MS/MS assay, J. Chromatogr., B: Anal. Technol. Biomed. Life Sci. 1210 (2022) 123432, https://doi.org/10.1016/j.jchromb.2022.123432.
[38] J.S. Woo, S.-H. Hwang, S. Yang, K.H. Lee, Y.S. Lee, J.W. Choi, J.-S. Park, J. Jhun, S.-H. Park, M.-L. Cho, Lactobacillus acidophilus and propionate attenuate Sjogren's syndrome by modulating the STIM1-STING signaling pathway, Cell Commun. Signal. 21 (1) (2023) 135, https://doi.org/10.1186/s12964-023-01141-0.